

Application of extended self similarity in turbulence

Siegfried Grossmann, Detlef Lohse, and Achim Reeh

Fachbereich Physik der Universität Marburg,

Renthof 6, D-35032 Marburg, Germany

(October 1, 2018)

From Navier-Stokes turbulence numerical simulations we show that for the extended self similarity (ESS) method it is essential to take the third order structure function *taken with the modulus* and called $D_3^*(r)$, rather than the standard third order structure function $D_3(r)$ itself. If done so, we find ESS towards scales larger than order $\sim 10\eta$, where η is the Kolmogorov scale. If $D_3(r)$ is used, there is no ESS. We also analyze ESS within the Batchelor parametrization of the second and third order longitudinal structure function and focus on the scaling of the transversal structure function. The Re-asymptotic inertial range scaling develops only beyond a Taylor-Reynolds number $Re_\lambda \gtrsim 500$.

I. INTRODUCTION

Extended self similarity (ESS, [1–3]) has been most useful in determining scaling exponents in experimental and numerical turbulent flow. In ESS, the p^{th} order longitudinal velocity structure function

$$D_p^L(r) = \langle [(\mathbf{u}(\mathbf{x} + \mathbf{r}) - \mathbf{u}(\mathbf{x})) \cdot \mathbf{e}_r^L]^p \rangle \quad (1)$$

is plotted against the third order structure function. Here, \mathbf{e}_r^L is the unit vector in \mathbf{r} direction; the unit vector \mathbf{e}_r^T used below is perpendicular to \mathbf{e}_r^L . The original motivation for picking the third order structure function was the Howard-v. Karman-Kolmogorov structure equation [4–6]

$$D_3^L(r) = -\frac{4}{5}\epsilon r + 6\nu \frac{d}{dr} D_2^L(r), \quad (2)$$

saying that in the inertial subrange (ISR) $D_3^L(r)$ scales like $D_3^L \propto r$ and therefore $D_p^L \propto r^{\zeta_p^L} \propto (D_3^L(r))^{\xi_p^L}$ has the same scaling exponent as a function of r or of D_3^L . However, because of the poor statistical convergence, rather than $D_3^L(r)$, the third order structure function $D_3^{*L}(r)$, calculated with the *modulus* of the velocity difference, is taken and it is argued [1, 3] that $D_3^{*L}(r)$ would also scale linearly with r in the ISR [7]. The resulting exponents, which in general have to be distinguished from the ζ_p^L 's [8], are denoted as ξ_p^L , defined by $D_p^L \propto (D_3^{*L})^{\xi_p^L}$, and they are found to be remarkable universal, i.e., independent of flow geometry and Reynolds number [9, 10].

Note that the degree of intermittency could be quantified by plotting $D_p^L(r)$ vs *any* structure function $D_q^L(r)$, (odd order moments taken with the modulus, $D_q^{*L}(r)$).

In this paper we would like to demonstrate that – beyond the mere practical reason of better statistics – it seems really essential for physical reasons to take $D_3^{*L}(r)$ rather than $D_3^L(r)$ to have ESS. We do so by examining ESS both for a full numerical simulation [11]

and for Batchelor’s parametrization of the structure function [12]. This parametrization will give us the opportunity to study finite Reynolds number Re effects. We will furthermore discuss the difference in scaling of the longitudinal as compared to the transversal structure functions.

We numerically solve the 3D incompressible Navier-Stokes equation on a N^3 grid with periodic boundary conditions. A pseudospectral code is used, the flow is forced on the largest length scales. For $N = 96$ we achieve a Taylor-Reynolds number $Re_\lambda = 110$; scales down to 3η are resolved; $\eta = \nu^{3/4}/\epsilon^{1/4}$ is the Kolmogorov length, ν the kinematic viscosity, ϵ the energy dissipation rate. Time integrations up to 150 large eddy turnovers are performed; the flow is locally isotropic to a high degree. More details on the numerical flow are given in ref. [11].

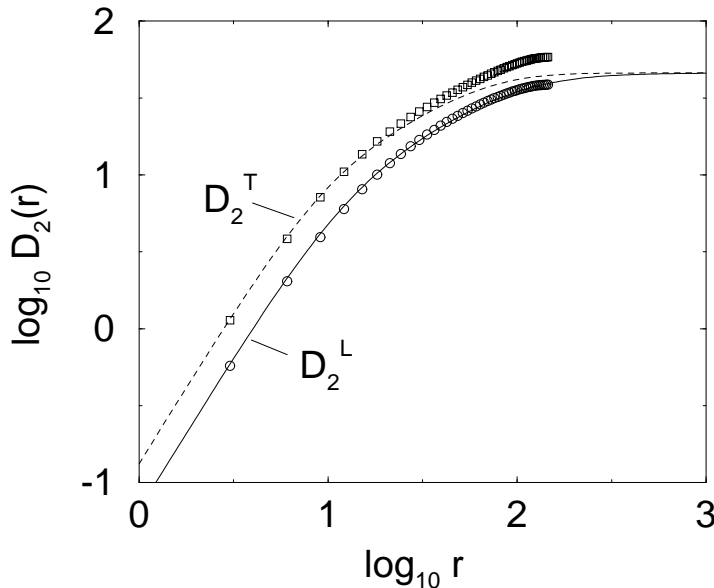


FIG. 1. Batchelor parametrization (3) (solid line) of the $N=96$ data for the longitudinal second order structure function $D_2^L(r)$ (numerical data: circles). We chose $a = 12.4\eta$ and $L = 108\eta$. Then we used eq. (6) to calculate $D_2^T(r)$ (dashed line) which poorly compares with the numerical data (squares) for r beyond the VSR.

II. BATCHELOR’S PARAMETRIZATION

The longitudinal second order structure function $D_2^L(r)$ is shown in figure 1. As in the whole paper, lengths are given in multiples of η and velocities in multiples of $(\epsilon\eta)^{1/3}$. An ISR scaling range is hardly developed because $Re_\lambda = 110$ is still small. The data are very well fitted by a parametrization of Batchelor’s type [12–16] with an additional large scale cutoff L [15, 17]

$$D_2^L(r) = \frac{\epsilon}{15\nu} \frac{r^2}{\left[1 + \left(\frac{r}{a}\right)^2\right]^{1-\zeta/2}} \frac{1}{\left[1 + \left(\frac{r}{L}\right)^2\right]^{\zeta/2}}. \quad (3)$$

Here, $\zeta = \zeta_2$ is the asymptotic ISR scaling exponents which from our [11] and others' [1–3, 6, 18] ESS analysis we take to be $\zeta = 0.70$. The only other free parameters are the viscous subrange - inertial subrange (VSR-ISR) crossover scale a and, of course, the large scale cutoff L . From a fit of eq. (3) to the present numerical data we find $a = 12.4\eta$ and $L = 108\eta$.

Note that we do not want to imply that all flow fields show a large scale saturation of type (3). However, those data (both numerical and experimental) we analyzed (see also [15, 17]) were well described by eq. (3). As eq. (3) guarantees an *analytic* behavior of both the correction term to r^2 on the small scale side and the correction term to $r = \text{const}$ on the large scale side we think that this is not accidental.

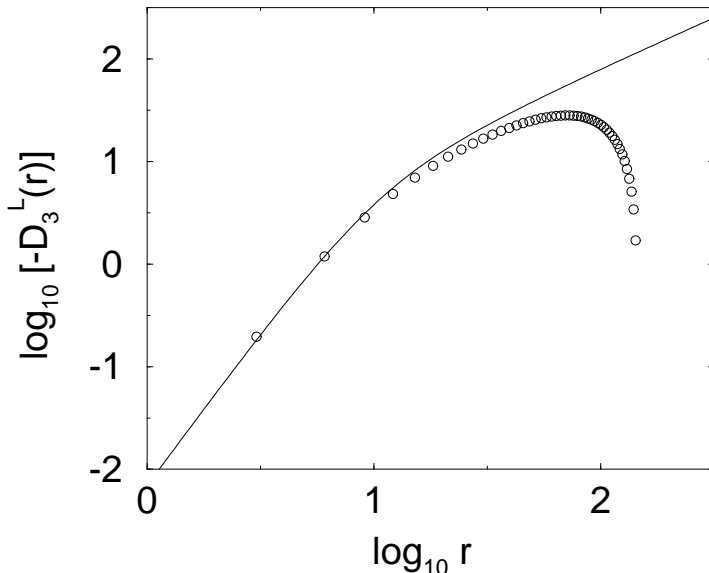


FIG. 2. Third order structure function from our numerical simulation (circles), compared with the one following from the Batchelor parametrization of $D_2^L(r)$ (full line). The Taylor-Reynolds number is $Re_\lambda = 110$.

With the outer length scale L we can define a Reynolds number $Re = u_{1,rms}L/\nu$. For very large Re the structure function (3) develops an ISR scaling law

$$D_2^L(r) = b^L(\epsilon r)^{2/3} \left(\frac{r}{L}\right)^{\delta\zeta_2}. \quad (4)$$

Here, $\delta\zeta_2 = \zeta_2 - 2/3$ is the scaling correction to classical scaling and b^L is often called the Kolmogorov constant. From our fit we have $b^L = \epsilon^{1/3}L^{\delta\zeta_2}a^{2-\zeta_2}/(15\nu) = 2.05$. This value well agrees with the data $b^L = 1.6 - 2.5$ known from the literature [4–6, 13, 19]; Sreenivasan [19] gives $b^L = 2.0 \pm 0.4$. Note that the full structure function $D_2(r) = 3D_2^L(r) + r\frac{\partial D_2^L}{\partial r}$ (for isotropic flow) asymptotically scales with a law of type (4), too; the prefactor is $b \approx 11b^L/3 = 6 - 9$. Alternatively, also $D_2(r)$ can be fitted by a Batchelor parametrization [13, 15] with similar quality [15].

Our motivation to employ Batchelor's parametrization (3) is to be able to *upscale* the second order structure function $D_2^L(r)$ to much larger Re (assuming that b^L and ζ are fixed

at $b^L = 2.0$ and $\zeta = 0.70$) and thereby get consistent data for the *transversal* second order structure function

$$D_p^T(r) = \langle [(\mathbf{u}(\mathbf{x} + \mathbf{r}) - \mathbf{u}(\mathbf{x})) \cdot \mathbf{e}_r^T]^p \rangle, \quad (5)$$

$p = 2$, and for the third order longitudinal structure function $D_3^L(r)$, which for isotropic, homogeneous, incompressible turbulence both follow from $D_2^L(r)$, namely through the relation

$$D_2^T(r) = D_2^L(r) + \frac{r}{2} \frac{d}{dr} D_2^L(r) \quad (6)$$

and through eq. (2), respectively.

To upscale $D_2^L(r)$ in eq. (3), we must know how the parameters a and L depend on the Reynolds number. If one accepts Sreenivasan's observations that neither the (asymptotic) dimensionless energy dissipation rate [20–22] $c_\epsilon = \epsilon L / u_{1,rms}^3$, nor the Kolmogorov constant b^L [19] (but note also ref. [23]) depend on the Reynolds number, one gets a weak dependence of the VSR-ISR crossover on the Reynolds number [22],

$$\frac{a}{\eta} = (15b^L)^{3/(4-3\delta\zeta)} \left(\frac{\eta}{L}\right)^{3\delta\zeta/(4-3\delta\zeta)}. \quad (7)$$

Once b^L , ζ , and Re are fixed, L and Re_λ can easily be obtained from above equations [21, 22]. With $D_2^L(\infty) = 2u_{1,rms}^2$ we get

$$\frac{L}{\eta} = \left(\frac{2}{b^L}\right)^{3/8} Re^{3/4}, \quad (8)$$

$$Re_\lambda = \frac{\sqrt{15}u_{1,rms}^2}{\sqrt{\nu\epsilon}} = \sqrt{15} \left(\frac{b^L}{2}\right)^{3/4} \sqrt{Re}. \quad (9)$$

Vice versa, once a and L are known, we obtain Re and Re_λ . For above values the result is $Re = 520$ and $Re_\lambda = 90$ for our numerical flow, in reasonable agreement to the direct numerical result $Re_\lambda = 110$. As we will see, the reason for the (modest) underestimation is that in the numerical flow there are correlations left at the largest length scales.

III. D_2^T AND D_3^L RESULTING FROM BATCHELOR'S PARAMETRIZATION

For $D_2^T(r)$ we find poor agreement between the curve evaluated from equation (6) and the numerically obtained values, see figure 1. The reason is that at $r \sim L$ there still is considerable correlation $\langle \mathbf{u}(x+r)\mathbf{u}(x) \rangle \neq 0$. More precisely, at the maximal meaningful distance r_{max} when employing periodic boundary conditions, namely, when r equals half of the periodicity length (here, $r_{max} \approx 146\eta$), we find $\langle u_j(\mathbf{x} + \mathbf{e}_r^L r_{max})u_j(\mathbf{x}) \rangle / \langle u_j^2(\mathbf{x}) \rangle \approx 0.25$ and $\langle u_j(\mathbf{x} + \mathbf{e}_r^T r_{max})u_j(\mathbf{x}) \rangle / \langle u_j^2(\mathbf{x}) \rangle \approx -0.15$ for $j = 1, 2$, or 3 . Therefore, $D_2^L(r_{max})$ is smaller and $D_2^T(r_{max})$ is larger than $2\langle u_j^2 \rangle$, which is the value the structure functions would take for perfect decorrelation between \mathbf{x} and $\mathbf{x} + \mathbf{r}_{max}$. Geometrically, the above correlations mean that there is an eddy with diameter $r \sim r_{max} \sim \pi L$ in the numerical flow. The possibility

of such large eddies is a consequence of the periodic boundary conditions (in contrast to boundary conditions which put the velocity to zero at the edge of the flow volume) and will also survive for larger Re_λ . Such a large scale eddy implies that the flow is *not* isotropic and homogeneous at the large scales and therefore it should be no surprise that equation (6), whose derivation requires isotropy and homogeneity, does not lead to good agreement with the data at large scales. Note that the same problem occurs in experimental flow, see e.g. figure 1a of ref. [24]. At the largest measured distance $r \approx 650\eta$ (for $Re_\lambda = 300$) it clearly is $D_2^T(r) > D_2^L(r)$, revealing a large scale eddy.

Also for $D_3^L(r)$ the agreement between the direct numerical values and those from the analytic equation (2), which assumes isotropy and homogeneity, is poor, see figure 2. The numerical structure function $D_3^L(r)$ bends down for large r as the velocity differences at large scales have Gaussian like statistics and consequently odd order moments almost vanish. This feature which is not described by eq. (2) is due to the boundary effects; more precisely, because there are no larger eddies than on the scale r_{max} which could provide correlations. In principle, this deficiency can be cured by adding a corresponding term to that equation as e.g. done in ref. [25].

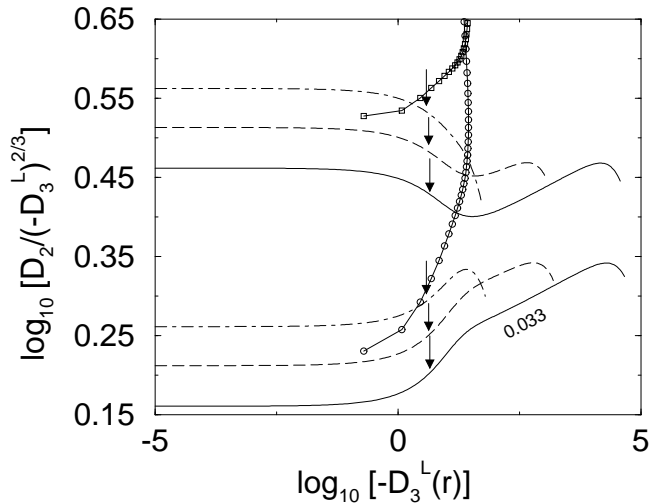


FIG. 3. Compensated ESS type plot $D_2/(D_3^L)^{2/3}$ vs D_3^L for the structure functions from the numerical simulation (circles: longitudinal; squares: transversal) and those following from the Batchelor parametrization (3) of D_2^L for Reynolds numbers $Re = 5.2 \cdot 10^2$ as in the numerical simulation, for $Re = 5.2 \cdot 10^4$, and for $Re = 5.2 \cdot 10^6$, corresponding to Taylor-Reynolds numbers of $Re_\lambda = 90$ (dot-dashed), $Re_\lambda = 900$ (dashed), and $Re_\lambda = 9000$ (solid); $\zeta = 0.7$, $b^L = 2.0$. The three lower curves are for the longitudinal structure functions, the three upper ones for the transversal ones. The arrows indicate 10η . The external length scales L are beyond the shown regimes.

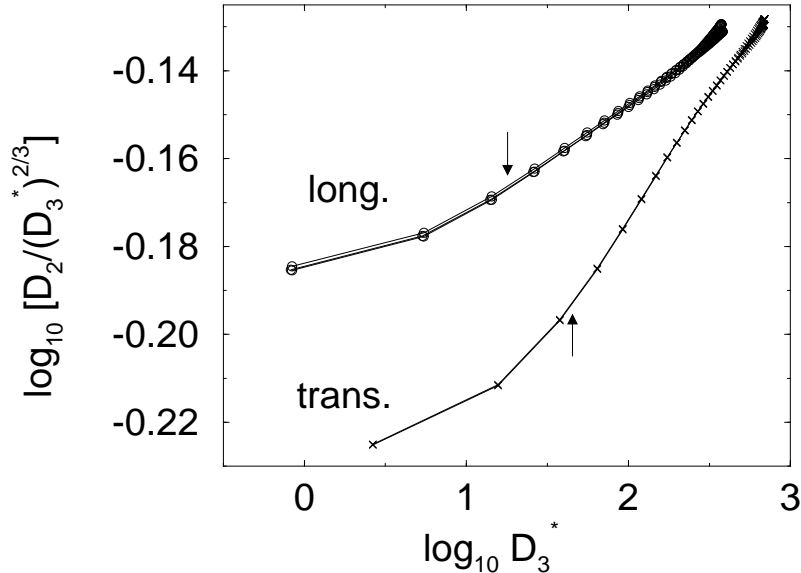


FIG. 4. Compensated ESS type plots $D_2^L / (D_3^{*L})^{2/3}$ vs D_3^{*L} (three different data sets for three different space directions which, however, agree very well) and $D_2^T / (D_3^{*T})^{2/3}$ vs D_3^{*T} (two data sets, also agreeing) for the numerical turbulence, $Re_\lambda = 110$. The arrows again indicate 10η ; the data points are for $r = 3\eta$, $r = 6\eta$, $r = 9\eta, \dots$, left to right.

IV. HOW TO APPLY ESS?

We now plot the second vs the third order structure function in a compensated ESS type plot, i.e., $D_2^L / (D_3^L)^{2/3}$ vs D_3^L , see figure 3. The scaling regime in the numerical simulation is by far too short to identify any scaling exponent. However, if we repeat this plot, but now with D_3^{*L} rather than D_3^L , ESS *is* seen, see figure 4. The reason is that D_2^L and D_3^{*L} have the same type of large scale saturation (i.e., becoming constant), whereas D_3^L has a different type of large scale behavior (namely, dropping to zero). We have to conclude that the extension of the scaling regime by using ESS is mainly an extension towards *large* scales. This even holds if Re_λ is so small that there is no ISR yet. The *small scale onset* of scaling still is around $r \sim 10\eta$, whether plotting D_2 vs D_3^{*L} or vs r , which is roughly the crossover scale $a \approx 12.4\eta$ found from employing eq. (3). In their numerical simulation Briscolini et al. [3] find an ESS extension down to $r \sim 7\eta$ (see figure 4 of their paper), roughly the same as the 10η reported here, but slightly smaller. As pointed out to us by R. Benzi, the origin of the slight difference may be that the small scale resolution in Briscolini et al. [3] is down to 1η , whereas here we only have a 3η resolution and the deviations in the structure functions due to the lower end of the resolution may influence the scaling exponents in a certain range of larger scales.

Our next point is to advocate *compensated* ESS plots for the visualization of intermittency effects. Already Meneveau [16] – see figure 1 of that paper – reveals how misleading an ESS plot D_p^L vs D_3^{*L} can be. Here, we demonstrate this in figure 5a which shows the original ESS plot D_2 vs D_3^* , only *pretending* better scaling than in figure 4. The reason is that in the VSR

the scaling exponent is $2/3$ for trivial reasons, a value which can hardly be distinguished by eye from the ISR value $2/3 + \delta\zeta_2 \approx 0.70$. To avoid this similarity of the VSR and ISR exponents, we prefer to use compensated ESS plots [11, 26].

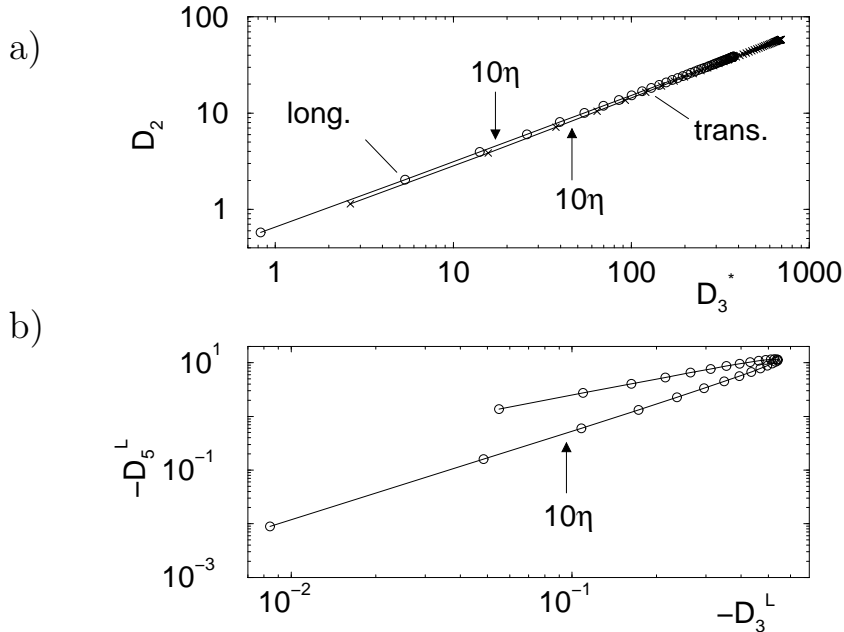


FIG. 5. (a) ESS plots $D_2(r)$ vs $D_3^*(r)$ for the longitudinal and transversal structure functions; $Re_\lambda = 110$. The data are the same as in the previous figure, where we showed the *compensated* ESS type plots, in which the different behavior in the VSR and the ISR is clearly visible. (b) ESS plots for $-D_5^L(r)$ vs $-D_3^L(r)$. In this figure the Taylor-Reynolds number is only 70, but we checked that the lack of ESS does not decrease with increasing Re_λ .

If one plots *local slopes* [8] as done in figure 6a it of course does not make any difference whether one takes them from compensated ESS plots or standard ESS plots. From figure 6a one notices that the ESS scaling $\xi_2^L \approx 0.69$ and $\xi_2^T \approx 0.72$ begins around 10η . From figure 6b one also notices that without ESS one could not deduce any scaling exponent at all for the small Reynolds number of our numerical calculation. ESS is thus useful already for the simple reason that a transition from a local slope of $2/3$ to roughly 0.70 is *shorter* than from a local slope 2 to roughly 0.70 .

As we will show now, there is no extended scaling regime towards scales much smaller than order $\sim 10\eta$, either, if one does ESS type plots with D_3^L instead of D_3^{*L} . We do so by plotting $D_2^L/(D_3^L)^{2/3}$ vs D_3^L with D_3^L following (via eq. (2)) from the Batchelor parametrization eq. (3) of D_2^L for various Re , see figure 3. We observe three regimes: The VSR without any scaling corrections (i.e., a horizontal line in figure 3), a crossover regime, corresponding to the range from $r \sim 1\eta$ to $r \sim 10\eta$, and only for large scales and large $Re \gtrsim 500$ the ISR scaling corrections $\delta\zeta_2 = 0.033$ can be identified.

To summarize this subsection: There seems to be ESS towards large scales, if the structure functions plotted against each other are both calculated with the moduli, i.e., have the same large scale saturation behavior. In particular, for the third order longitudinal structure function this means that it is essential to take D_3^{*L} rather than D_3^L and to clearly distinguish

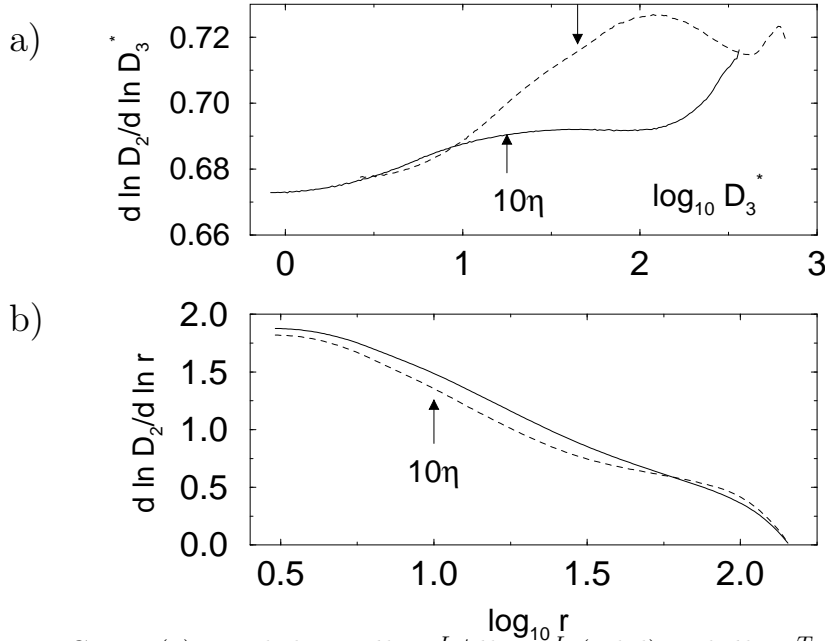


FIG. 6. (a) Local slopes $d \lg D_2^L / d \lg D_3^{*L}$ (solid) and $d \lg D_2^T / d \lg D_3^{*T}$ (dashed) of the curves in figure 5a. The arrows indicate 10η .
 (b) Local slopes $d \lg D_2^L / d \lg r$ (solid) and $d \lg D_2^T / d \lg r$ (dashed) of the numerical data curves $D_2^{L,T}(r)$ in figure 1.

between the ζ_p and ξ_p exponents. This was already stressed by Stolovitzky and Sreenivasan [8], see in particular their figures 2 and 4 where they compare local slopes of D_8^L vs. D_3^L and D_3^{*L} .

The natural question to ask is: Is there also ESS for odd order structure functions (calculated *without* the modulus) plotted against each other? In figure 5b we plot $-D_5^L$ vs $-D_3^L$. No ESS towards large scales is seen. It seems that odd and even order moments obey fundamentally different types of statistics. This finding may be connected to Herweijer and van der Water's finding [27] that ζ_p for *odd* p (calculated from $D_p^L(r) \propto r^{\zeta_p}$) are *smaller* than expected from an extrapolation of the neighboring $\zeta_{p\pm 1}$ (for which the $p \pm 1$ are even). A difference between the ζ_p for odd and even p was also found by Stolovitzky et al. [8, 14]; however, for the flow analyzed in that references the ζ_p for odd p are *larger* than expected from the extrapolation.

We do not understand *why* nonuniversal forcing and large scale boundary effects roughly cancel out in even order structure functions but not in odd order ones (calculated without the modulus). With a more elaborate technique it may even be possible to extract nonuniversal properties also from ESS plots of even structure functions. On the other hand, we cannot exclude that there is more universality in *decaying* turbulence where less anisotropy through the forcing and the boundaries is felt.

V. LONGITUDINAL VS TRANSVERSAL STRUCTURE FUNCTIONS

Next, we focus on the difference in the scaling between longitudinal and transversal structure functions, $D_p^L(r) \propto r^{\zeta_p^L}$ and $D_p^T(r) \propto r^{\zeta_p^T}$, respectively. Recently, different degrees of intermittency for longitudinal and transversal fluctuations were reported in some experiments [24, 28, 29] and numerical simulations on decaying turbulence [30]. We confirmed these findings for statistically stationary turbulence [11] (see also ref. [31]). More precisely, it were the ESS type scaling exponents ξ_p^L and ξ_p^T , defined by $D_p^L \propto (D_3^{*L})^{\xi_p^L}$ and $D_p^T \propto (D_3^{*T})^{\xi_p^T}$, which are clearly different; we found $\delta\xi_6^L = 0.21 \pm 0.01$ and $\delta\xi_6^T = 0.43 \pm 0.01$ for the deviations from the mean field value $\xi_6 = 2$ [11].

One would be tempted to conclude that the best way to see a deviation in scaling between D_p^L and D_p^T would be to plot the *ratio* D_p^T/D_p^L vs r (or vs D_3^L). According to eq. (6), $D_2^T(r)$ and $D_2^L(r)$ scale the same in the ISR, i.e., the ratio should be constant. However, figure 7a seems to imply different scaling of $D_2^L(r)$ and $D_2^T(r)$.

The reason for this apparent discrepancy is that the argument of equal scaling of $D_2^L(r)$ and $D_2^T(r)$ is only valid if both structure functions scale individually. This is not the case in the transition ranges or if there is not any ISR yet. Here, the Reynolds number achieved in the full simulation is by far too small to give the asymptotic (ISR) scaling. In figure 7b we redo this type of plot, but now within the Batchelor parametrization for which we can achieve arbitrarily large Re_λ . Only if $Re_\lambda \gtrsim 500$ a plateau starts to develop, showing the onset of the asymptotically correct ISR behavior. To reliably determine scaling exponents from the plateau, one would need at least Taylor-Reynolds numbers ~ 1000 and beyond. For $Re_\lambda \sim 100$ there is a fake scaling law with an apparent exponent of -0.14 , which has nothing to do with inertial range scaling.

Going back to eqs. (3) and (6), this behavior can be understood. In the VSR we must have $D_2^T/D_2^L = 2$ (because of eq. (6) and $D_2^L \propto r^2$) and in the ISR we have $D_2^T/D_2^L \approx 4/3$ (because of eq. (6) and roughly $D_2^L \propto r^{2/3}$), just as seen in figure 7b. The crossover between these two regimes is about a decade. The same can be seen from figure 3 where besides $D_2^L/(D_3^L)^{2/3}$ we also plotted $D_2^T/(D_3^T)^{2/3}$ vs D_3^L . In the crossover regime where the former curve bends up, the latter bends down. Again, only for $Re_\lambda \gtrsim 500$ the asymptotic scaling exponent $\delta\zeta_2^L = \delta\zeta_2^T = 0.033$ starts to be observable.

The same finite Re_λ effects which we discussed for the 2nd order structure functions, where D_2^L and D_2^T are *known* to have the same scaling, will *hinder* to determine scaling exponents vs r (or vs D_3^L) in higher order structure functions for too low $Re_\lambda \lesssim 500$.

VI. SUMMARY

To conclude, we confirmed the finding of Briscolini et al. [3] that ESS does not extend to scales below order $\sim 10\eta$. We furthermore showed from calculations with the Batchelor parametrization that scaling exponents ζ_p calculated from structure functions plotted vs r (or vs D_3^L) can only securely be measured for Re_λ sufficiently larger than 500. For smaller Re_λ , in particular for all present day numerical simulations, one is restricted to *relative*, ESS type scaling exponents ξ_p calculated from ESS type plots $D_p^{*L}(r)$ vs $D_q^{*L}(r)$ and $D_p^{*T}(r)$ vs $D_q^{*T}(r)$, whereby it is essential to calculate the structure functions from the moduli of the

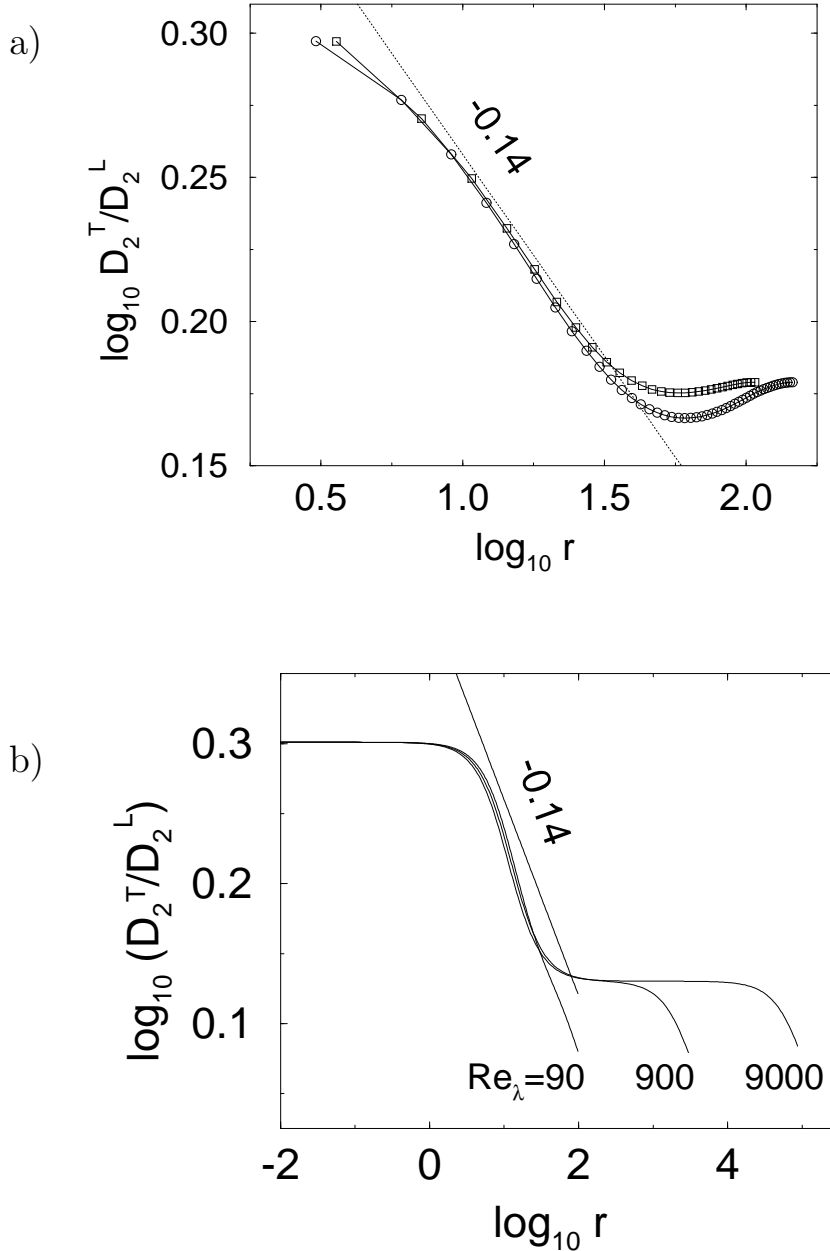


FIG. 7. (a) The ratio $D_2^T(r)/D_2^L(r)$ vs r for the numerical data of a $Re_\lambda = 110$ (circles) and a $Re_\lambda = 70$ (squares) simulation. *Erroneously*, one may deduce *different* scaling of $D_2^L(r)$ and $D_2^T(r)$ because the ratio depends on r . We also included an apparent slope of -0.14 .

(b) $D_2^T(r)/D_2^L(r)$ as a function of r for the Batchelor parametrization (3) for Taylor-Reynolds numbers of $Re_\lambda = 90$, $Re_\lambda = 900$, and $Re_\lambda = 9000$. The plateau in the ISR (at roughly $lg(4/3) = 0.125$) expected for isotropic homogeneous flow only starts to develop for as large Re_λ as $Re_\lambda \sim 500$. The VSR plateau is at $lg 2 = 0.30$. The r -dependent intermediate range characterizes the transition between the VSR and the ISR. The slope is related to its width and the different heights of the two plateaus. As a side remark we mention that in this plot one can also notice the Re_λ dependence of the VSR-ISR crossover a , cf. eq. (7): the transition range is shifted towards smaller r with increasing Re_λ .

velocity differences. For odd order moments, calculated *without* taking the modulus, ESS does not hold in the presented numerical simulation.

Acknowledgements: We thank Roberto Benzi and Luca Biferale for very helpful comments on the manuscript. Support for this work by the Deutsche Forschungsgemeinschaft (DFG) under grant SBF185 and by the German-Israel Foundation (GIF) is gratefully acknowledged. The HLRZ Jülich supplied us with computer time.

e-mail addresses:

grossmann_s@physik.uni-marburg.de
lohse@stat.physik.uni-marburg.de
reeh@mailier.uni-marburg.de

-
- [1] R. Benzi *et al.*, Phys. Rev. E **48**, R29 (1993).
 - [2] R. Benzi, S. Ciliberto, C. Baudet, and G. R. Chavarria, Physica D **80**, 385 (1995).
 - [3] M. Briscolini, P. Santangelo, S. Succi and R. Benzi, Phys. Rev. E **50**, R1745 (1994).
 - [4] A. S. Monin and A. M. Yaglom, *Statistical Fluid Mechanics* (The MIT Press, Cambridge, Massachusetts, 1975).
 - [5] M. Nelkin, Advances in Physics **43**, 143 (1994).
 - [6] U. Frisch, *Turbulence* (Cambridge University Press, Cambridge, 1995).
 - [7] Roberto Benzi (priv. communication) communicated us that for an experimental flow in a regime where no forcing is felt this indeed were the case. Other authors find differences; e.g., J. A. Herweijer (Ph.D. thesis, University of Eindhoven, 1995) finds $D_3^L(r) \propto r^{1.035 \pm 0.005}$ and $D_3^{*L}(r) \propto r^{1.055 \pm 0.005}$ for a wind tunnel measurement.
 - [8] G. Stolovitzky and K. R. Sreenivasan, Phys. Rev. E **48**, R33 (1993).
 - [9] A. Arneodo et al., Europhys. Lett. **34**, 411 (1996).
 - [10] F. Belin, P. Tabeling, and H. Willaime, Physica D **93**, 52 (1996).
 - [11] S. Grossmann, D. Lohse, and A. Reeh, “Different intermittency for longitudinal and transversal turbulent fluctuations”, submitted to Phys. Fluids (chao-dyn/9704014).
 - [12] G. K. Batchelor, Proc. Camb. Philos. Soc. **47**, 359 (1951).
 - [13] H. Effinger and S. Grossmann, Z. Phys. B **66**, 289 (1987).
 - [14] G. Stolovitzky, K. R. Sreenivasan, and A. Juneja, Phys. Rev. E **48**, R3217 (1993); L. Sirovich, L. Smith, and V. Yakhot, Phys. Rev. Lett. **72**, 344 (1994).
 - [15] D. Lohse and A. Müller-Groeling, Phys. Rev. Lett. **74**, 1747 (1995).
 - [16] Ch. Meneveau, Phys. Rev. E **54**, 3657 (1996).
 - [17] D. Lohse and A. Müller-Groeling, Phys. Rev. E **54**, 395 (1996).
 - [18] R. Benzi *et al.*, Physica D **96**, 162 (1996).
 - [19] K. R. Sreenivasan, Phys. Fluids **7**, 2778 (1995).
 - [20] K. R. Sreenivasan, Phys. Fluids **27**, 1048 (1984).
 - [21] D. Lohse, Phys. Rev. Lett. **73**, 3223 (1994).
 - [22] S. Grossmann, Phys. Rev. E **51**, 6275 (1995); G. Stolovitzky and K. R. Sreenivasan, Phys.

- Rev. E **52**, 3242 (1995).
- [23] A. Praskovsky and S. Oncley, Phys. Fluids A **6**, 2886 (1994).
 - [24] J. Herweijer and W. van der Water, in *Advance in Turbulence V*, edited by R. Benzi (Kluwer Academic Publishers, New York, 1995), p. 210.
 - [25] V. Yakhot, Phys. Rev. Lett. **69**, 769 (1992).
 - [26] S. Grossmann, D. Lohse, and A. Reeh, Phys. Rev. Lett. **77**, 5369 (1996).
 - [27] J. Herweijer and W. van de Water, Phys. Rev. Lett. **74**, 4651 (1995).
 - [28] W. van de Water and J. Herweijer, “High order structure functions of turbulence”, preprint, Eindhoven 1996; W. van de Water and J. A. Herweijer, Phys. Scripta T67, 136 (1996).
 - [29] R. Camussi and R. Benzi, Phys. Fluids **9**, 257 (1997).
 - [30] O. N. Boratav and R. B. Pelz, Phys. Fluids **9**, 1400 (1997).
 - [31] S. Chen, K. R. Sreenivasan, M. Nelkin, and N. Cao, “A refined similarity hypothesis for transversal structure functions”, preprint (1997).